

## EAS observation conditions monitoring in the SPHERE-2 balloon experiment

---

**Bonvech Elena,<sup>a,\*</sup> Chernov Dmitry,<sup>a</sup> Finger Miroslav,<sup>b,c</sup> Finger Michael,<sup>b,c</sup> Galkin Vladimir,<sup>a,d</sup> Podgrudkov Dmitry,<sup>a,d</sup> Roganova Tatiana<sup>a</sup> and Vaiman Igor<sup>a,e</sup>**

<sup>a</sup>*Skobeltsyn Institute for Nuclear Physics, M.V. Lomonosov Moscow State University, Moscow 119991, Russia*

<sup>b</sup>*Charles University, Prague, Czech Republic*

<sup>c</sup>*International Intergovernmental Organization Joint Institute for Nuclear Research, Dubna, Russia*

<sup>d</sup>*Faculty of Physics, Lomonosov Moscow State University, Moscow, Russia*

<sup>e</sup>*Institute for Nuclear Research (INR) of the Russian Academy of Sciences, Moscow, Russia*

*E-mail: [bonvech@yandex.ru](mailto:bonvech@yandex.ru), [chr@dec1.sinp.msu.ru](mailto:chr@dec1.sinp.msu.ru)*

The SPHERE project studies primary cosmic rays by registration of the extensive air showers (EAS) Cherenkov light reflected from the snow covered ground. The SPHERE project is the first successful implementation of this new EAS detection method, first proposed by Alexander Chudakov and first implemented by Rem Antonov. The SPHERE-2 experiment was designed for studies in the 10–1000 PeV energy range. The detector was lifted by a balloon to altitudes of up to 900 m above the snow covered surface of Lake Baikal. Measurements were performed in 2011–2013.

Here we present an overview of the SPHERE-2 detector telemetry monitoring systems along with the analysis of the measurements conditions including atmosphere profile. The analysis of the detector state and environment atmosphere conditions monitoring provided various cross-checks of the detector calibration, positioning, and performance.

\*\*\* 27th European Cosmic Ray Symposium - ECRS \*\*\*

\*\*\* 25-29 July 2022 \*\*\*

\*\*\* Nijmegen, the Netherlands \*\*\*

---

\*Speaker

## 1. Introduction

The SPHERE-2 detector was designed for the primary cosmic ray (PCR) studies in the 10–1000 PeV energy range. The SPHERE experiment is a first successful implementation of a new EAS registration method — registration of the reflected Cherenkov light using an compact aerial-based detector.

This method was first proposed by A.E. Chudakov [1] and first successfully implemented by R.A. Antonov [2–4]. The SPHERE-2 detector registered extensive air showers (EAS) on relatively large area. It represents a small size compact detector with all the advantages of such a setup: a complex topological trigger conditions prior to writing data to storage thus increasing the maximum operational count rate; direct on-line calibration system; high mobility with lower operational costs etc.

The general overview of the SPHERE-2 experiment can be found in [5], and the detailed description of the detector electronics is given in [6]. The SPHERE-2 balloon detector optics comprised a 1.5 m diameter spherical mirror with a 109 photomultiplier tube (PMT) mosaic near mirror's focus. The detector was lifted by a balloon to altitudes of up to 900 m above the snow covered surface of Lake Baikal.

## 2. Telemetry monitoring

In normal conditions the detector axis should be oriented vertically for it to observe the surface exactly below it. However, during flights the detector was attached to the balloon in a single point and swung and rotated freely. The SPHERE-2 detector's position and inclination depend on the wind conditions near the detector.

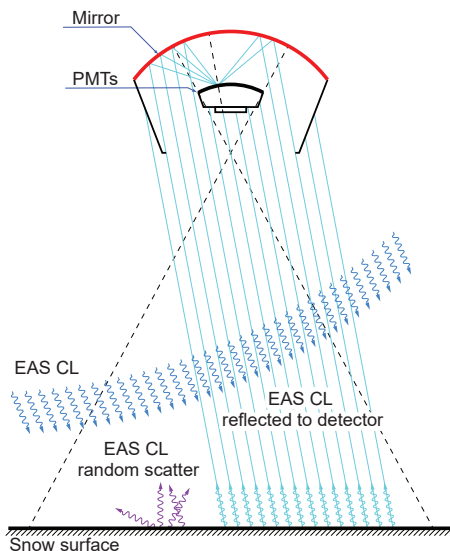


**Figure 1:** SPHERE-2 experiment scheme. Detector was elevated above the snow covered surface of the Baikal Lake by the balloon. Detector collected Cherenkov light reflected from the lake snow.

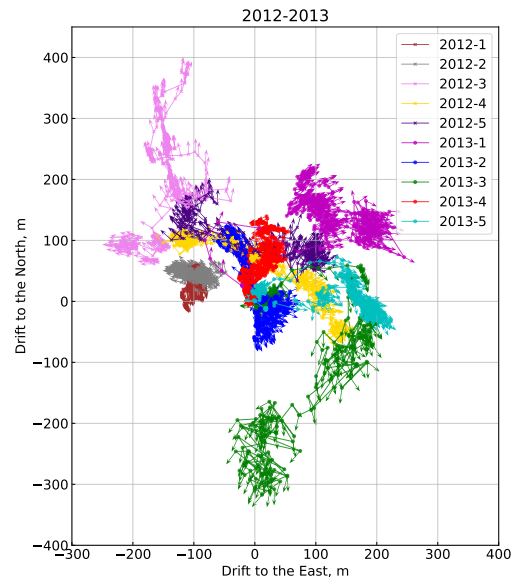


**Figure 2:** The SPHERE-2 detector drift in 2012-2013. Points indicate detector position in 1 min intervals, arrows indicate the detector magnetometer orientation.

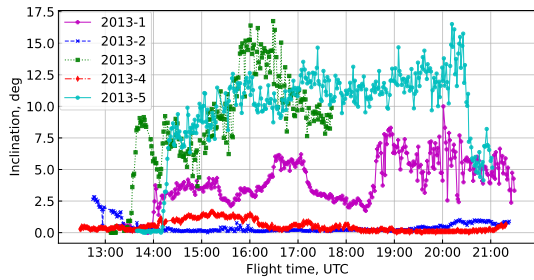


**Figure 3:** The detector inclination according to the inclinometer sensor during several flights of 2013.

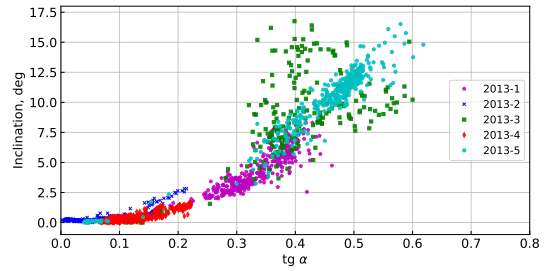


**Figure 4:** Detector inclination against the ratio of detector drift from the start point to the detector altitude.

There were many telemetry sensors onboard of the SPHERE-2 detector. The Garmin 16xHVS GPS sensor provided coordinates and an elevation above sea level. Figure 2 shows the detector position according to the GPS data in two seasons 2012 and 2013 in 1 min intervals. The launch point was located at zero coordinates. The detector drifted from the start point under wind. However, the wind was stable or slowly variable during the flight. The digital compass measured the detector's orientation relative to the Earth's magnetic field with 2.5 degree precision. The arrows in Figure 2 indicate the detector's compass orientation, as it changed slowly over time.

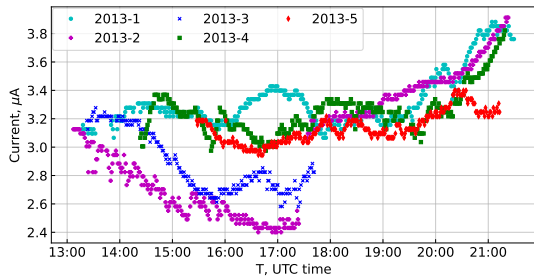
The inclinometer installed under the PMTs measured inclination of detector in two orthogonal planes. The resulting inclination angle is shown in Figure 3 for flights of the 2013 run. The maximal inclination angle recorded was about  $17^\circ$ . In Figure 4, the detector inclination angle is shown depending on the ratio of the drift distance from the starting point to the flight altitude (roughly the tangent of the balloon tether angle) for all experimental flights. This ratio, as was expected, depends on wind strength which, in turn, influences the detector inclination angle. Strong fluctuations in flight 2013-3 (green squares) coincided with a weather change (strong wind gusts, temperature and pressure change, appearance of clouds), which resulted in early detector landing due to bad flight conditions. The wind conditions in the experiment runs were quite constant for most of the time, and the balloon position was rather stable and varied slowly.

Figure 5 shows the anode current of the detector mosaic central PMT for the flights of 2013 run. In general, the PMT current variations during the observations followed the variation of the background illumination of the snow.

To monitor the air condition two identical barometers were used, one of them was installed on the apparatus, the other one remained on the ice at the launch point. The surrounding air temperature and pressure from the detector barometer are presented in Figures 6 and 7.

### 3. GPS altitude correction

The detector observation area depends on the detector altitude  $H$  as a square function. The detector altitude was measured by GPS module, see Figure 7 and was verified by the pressure sensor. However it was noticed that after rapid changes in altitude due to the balloon ascent or descent, the GPS registered height lagged behind the corresponding pressure change and varied in a smoothed fashion, most probably, due to the GPS internal error correction algorithm.



**Figure 5:** Central PMT current in flights of 2013 run.

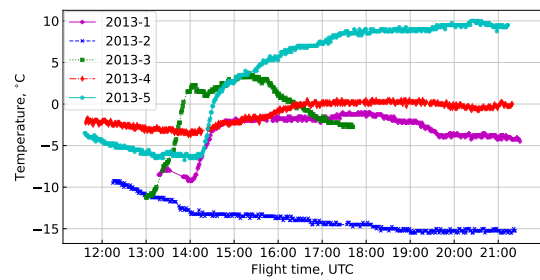


**Figure 6:** Air temperature near the PMT mosaic during 2013 flights.

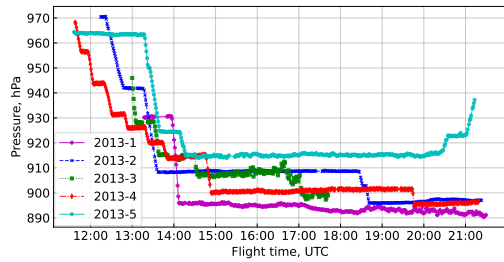


**Figure 7:** Air pressure according to the barometer sensor data during 2013 flights.

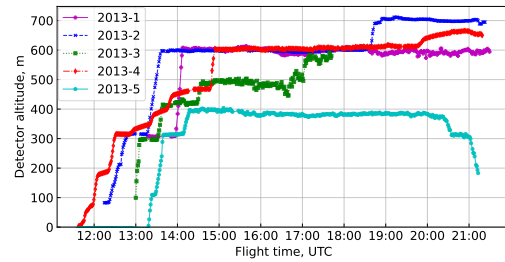


**Figure 8:** Detector elevation according to the GPS sensor during 2013 flights.

To provide the correct altitude the data from GPS module, onboard barometer and ground barometer at launchpad was used. One can expect GPS height  $h$  and difference between surface level and balloon level pressures  $\Delta p = (p_{surf} - p_{air})$  to behave consistently because of pressure dependence on altitude. Other major parameters that affect pressure, such as temperature and humidity, affect both  $p_{surf}$  and  $p_{air}$  and their effects at least partially cancel each other out in  $\Delta p$ .

This expected consistent behavior is observed when balloon altitude is generally stable. On Figure 9 such region is shown in the 2013-3 data. Parameters  $h$  and  $\Delta p$  are normalized and filtered with high-pass digital Butterworth filter with cutoff frequency 0.83 mHz ( $T = 20$  min). It's clear that short-term fluctuations of GPS altitude and pressure difference are in good correlation. Correlation coefficient is 0.96 for this data and no less than 0.9 for all other flights' stable altitude regions filtered the same way. From this we conclude that GPS and barometer data are reliable when altitude is relatively stable and surface-air pressure difference directly indicates rapid fluctuations in height.

However, there are regions in data in which parameters  $h$  and  $\Delta p$  behave rather inconsistently. In Figure 10 such region in the flight 2013-4 data is shown (these data are scaled without any filtering). When barometer data change rapidly indicating rapid balloon ascend the GPS data starts to change with significant delay and in unnatural smoothed fashion. Such regions in GPS data are observed during almost every abrupt changes in balloon altitude. We believe that this is due to some internal algorithm of the GPS module. Module was designed for naval and small aircraft use so it probably handles rapid change in altitude with no ground speed as an error and tries to smooth it out.

Internal algorithm of the GPS module is not available so we've made an attempt to reconstruct correct height data based on pressure measurements which are found to be directly linked to altitude. After we manually identified smoothed regions such as that shown in Figure 10 we

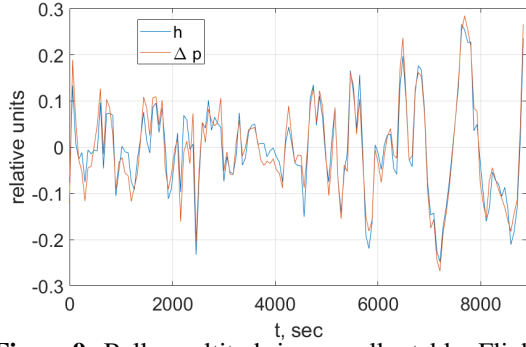


**Figure 9:** Balloon altitude is generally stable. Flight 2013-3 data.

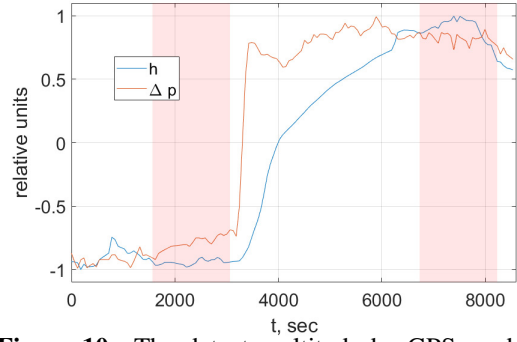


**Figure 10:** The detector altitude by GPS module and reconstructed with pressure sensor data. Flight 2013-4, the elevation phase.

picked two adjacent regions of relatively stable altitude before and after it (example of these regions is shown in Figure 10 with red bands). In these regions pressure and GPS height data behave consistently (in terms of filtered short-term fluctuations) so we assumed that both measurements are valid. Between these regions the GPS height data are invalid and to be replaced with ‘barometric’ height logarithmic interpolation in the form of  $h - h_0 = -a \ln(p/p_0)$ . Obtained coefficient  $a$  describes local atmosphere and is close to widely adopted value of 8 km.

The correction was made for a total of 220 min of measurements, where 68 triggers were registered.

#### 4. Atmosphere profile

After the corrections were applied to GPS altitudes, the atmosphere density profiles were reconstructed. Direct measurements with an on-board barometer and thermometer were taken only at altitudes below 900 m above the ice; therefore, information about higher atmospheric conditions was not available. To obtain the best extrapolation of this data, we had to use a set of parameterized atmospheres provided by the CORSIKA software [7] version 7.5600.

The CORSIKA code provides 26 atmosphere models pertinent to different seasons and locations. We used the following equations to derive the mass overburden  $t$  and density  $\rho$  from the measured pressure  $p$  and temperature  $T$  data:

$$t = \frac{p}{g}, \quad \rho = \frac{pM}{RT} \quad (1)$$

Here,  $g$  is the gravitational acceleration,  $M$  is the average molar mass of air, and  $R$  is the gas constant.

Mass overburden data were reconstructed from atmospheric pressure measurements and air density was estimated based on both air pressure and temperature around the balloon. Calculated experimental points for  $t$  and  $\rho$  for each flight are shown in Figure 11 and in Figure 12, respectively. CORSIKA atmospheres are shown with solid lines. The profile that was adopted prior to the actual measurements for the preliminary modeling (atmosphere model 11) is shown by the red line. From this comparison, it may be seen that the previously picked atmosphere is inconsistent

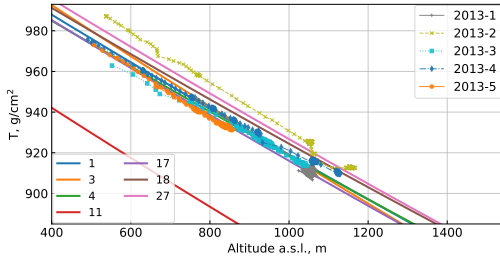


**Figure 11:** Mass overburden versus altitude experimental data (points) in each flight of 2013 run and CORSIKA profiles (solid lines with corresponding models numbers).

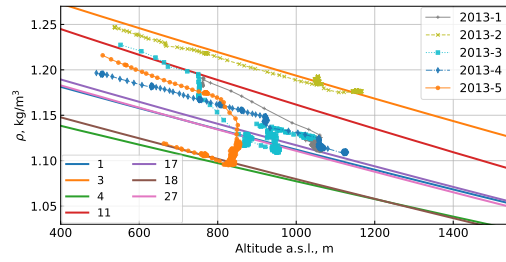


**Figure 12:** Density versus altitude experimental data (points) in each flight and CORSIKA models density profiles (solid lines) same as in Figure 11).

with our experimental data for  $t$  in terms of absolute values, but their derivatives lie relatively close. CORSIKA atmosphere model 11 was used for modeling and estimations at the SPHERE-2 experiment planning stage. However, our data show that this choice was not ideal.

The use of experimental points in  $t$  or  $\rho$  cannot provide a reasonable choice of the model, but only give a clue as to what the model should be. A full-fledged choice must include data on the vertical profile of the atmosphere up to altitudes of at least 10 km above the lake because Cherenkov light mostly comes from this layer. Still some conclusions on the atmosphere model effect on primary energy and mass estimates can be made by comparing the artificial showers simulated for different models.

Artificial showers initiated by 10 PeV protons were modeled using CORSIKA for atmosphere model 11 resembling the experimental  $\rho$  curves, as well as for models 3 and 4 roughly following the data on  $t$ . In Figures 13 and 14 the ratios of Cherenkov photons local densities for showers developed in different atmospheres are presented. Substantial changes of the atmosphere model affect the total number of Cherenkov photons and the estimates of primary energy by no more than 5% on average. However, the mass-sensitive parameter based on the Cherenkov light lateral distribution function steepness [8] is extremely sensitive to the atmosphere model.

## 5. Conclusions

The SPHERE-2 detector which operated in 2011–2013 had a large array of supplementary sensors that allowed to control and later reconstruct the state of the detector and measurement conditions.

For the reflected Cherenkov light registration method the information on detector position and orientation is crucial. Their values were measured with good precision. The altitude of the detector above the observation surface was recorded using GPS, the readings of which were checked and, if necessary, corrected according to the barometer data.

Measurements of air pressure and temperature during flights gave information on the atmosphere profile that will allow to introduce correct atmospheric models into analysis and to account their impact on the mass composition analysis results. Availability of the data on the atmospheric state at the moment of the EAS detection allows more accurate primary mass reconstruction. Carrying out daily measurements of the state of the atmosphere in different layers of the atmosphere is

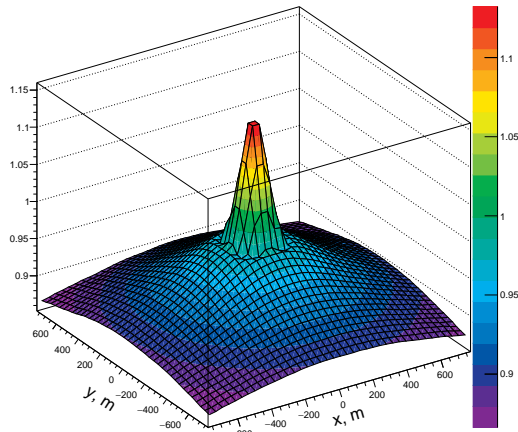


**Figure 13:** Sample mean Cherenkov light lateral distribution ratio for CORSIKA atmosphere model pair 11/3. Bin size  $50\text{ m} \times 50\text{ m}$ . 10 PeV primary protons. Zenith angle 15 deg. Sample volume 30 events.

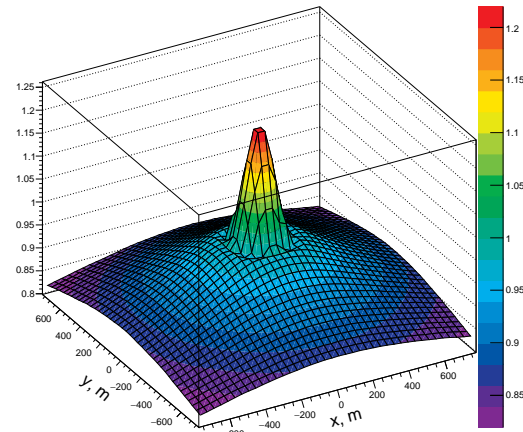


**Figure 14:** Sample mean Cherenkov light lateral distribution ratio for CORSIKA atmosphere model pair 11/4. Bin size  $50\text{ m} \times 50\text{ m}$ . 10 PeV primary protons. Zenith angle 15 deg. Sample volume 30 events.

critical for reconstructing the composition of cosmic rays. This is important not only for balloons, but also for ground based installations.

## References

- [1] A. Chudakov, *A possible method to detect EAS by the Cherenkov radiation reflected from the snowy ground surface. (in Russian)*, in *Experimental methods of studying cosmic rays of superhigh energies: Proc. All-Union Symposium*, vol. 620, pp. 69–72, 1972.
- [2] R. Antonov and et al, *Installation for measuring the primary energy spectrum of cosmic rays in the energy range above  $10^{15} - 10^{16}$  eV*, *Proc. 14th ICRC (München)* **9** (1975) 3360.
- [3] Antonov, R. A.; Ivanenko, I. P.; Kuzmin, V. A., *Simulating an apparatus for examining the primary cosmic-ray spectrum at  $10^{15} - 10^{20}$  eV*, *Bulletin of Academy of Sciences of the USSR, Physical series* **50** (1986) 136.
- [4] R. Antonov and et al, *Primary cosmic ray spectrum measured using cherenkov light reflected from the snow surface*, *Proceedings of the 25th ICRC (Durban)* **4** (1997) 149.
- [5] R. Antonov, T. Aulova, E. Bonvech, V. Galkin and et al, *Detection of reflected Cherenkov light from extensive air showers in the SPHERE experiment as a method of studying superhigh energy cosmic rays*, *Physics of Particles and Nuclei* **46** (2015) 60.
- [6] R. Antonov, E. Bonvech, D. Chernov, T. Dzhatdov, M. Finger, M. Finger et al., *The SPHERE-2 detector for observation of extensive air showers in 1 PeV–1 EeV energy range*, *Astroparticle Physics* **121** (2020) 102460.

- [7] D. Heck, J. Knapp, J.N. Capdevielle, G. Schatz and T. Thouw, *CORSIKA: A Monte Carlo code to simulate extensive air showers*, (1998) Report FZKA.
- [8] R.A. Antonov, T.V. Aulova, E.A. Bonvech, D.V. Chernov, T.A. Dzhatdoev, M. Finger et al., *Event-by-event study of CR composition with the SPHERE experiment using the 2013 data*, *Journal of Physics Conference Series* **632** (2015) 012090.